Tetrahedron Vol 47, No 34, pp. 7135-7156, 1991
Printed in Great Britain

0040-4020/91 $3 00+ 00

Synthesis of Tetrameric Branched RNA-DNA Conjugate & Branched-RNA Analogue & Their Comparative Conformational Studies By 500 MHz NMR Spectroscopy

András Foldesi+, Peter Agback, Corin Glemarec & Jyoti Chattopadhyaya*

Department of Bioorganic Chemistry, Box 581, Biomedical Center,
University of Uppsala, S-751 23 Uppsala, Sweden

(*Received in UK* 17 *May* 1991)

Key Words Branched RNA, DNA, Synthesis, NMR, Conformation

Abstract We report herein the unambiguous synthesis of pure tetrameric branched oligonucleotides $A3'p5'G^{2'p5'[dC]}_{3'p5'C}$ *(13) found naturally in gram-negative bacterium Stigmatella aurantiaca, and corresponding branched RNA analogue* $A3'p5'G^{2'p5'C}_{3'p5'C}$ *(14) The conformational features of branched tetramers 13 and 14 have been elucidated and compared by assesing temperature- and concentration-dependent* ^1H *and* ^{31}P *chemical shifts, (C2'-exo and C3'-endo)* $\rightleftarrows$ *(C2'-endo, C3'-exo) equilibrium, and equilibrium amongst staggered* γ *and* β *rotamers using various 2D homo- and heteronuclear correlation, NOESY and ROESY experiments by 500 MHz NMR spectroscopy Subsequently the conformational features of 13 and 14 have been compared with those of* $A^{2'p5'G}_{3'p5'C}$ *(ref 19) and* $U3'p5'A^{2'p5'G}_{3'p5'C}$ *(ref 24) found as the branch-point in the lariat formed in the pre-mRNA processing reaction (Splicing) These studies have clearly shown that (1) the intramolecular geometries of both 13 and 14 are dominated by stacking along the axis A3'→ 5'G2'→5'dC(C), but the RNA-DNA conjugate 13 has a more defined tertiary structure than that of 14, (2) these branched tetramers tend to associate intermolecularly above ~2 mM concentration producing an aggregate which is vertically stacked along the axis A3'→5'G2'→5'dC(C), (3) the G2'→ 5'dC(C) stacking and the predominant S conformation of branch-point G found in 13 and 14 suggest that their structures are quite different from the ones found for* $U3'p5'A^{2'p5'G}_{3'p5'C}$ *(ref 24) Note however that the structures found for 13 and 14 are reminiscent of A2'→5'G stacking found in the branched trimer* $A^{2'p5'G}_{3'p5'C}$ *(ref 19)*

The 5'-end of the multiple single-stranded linear DNA (msDNA) of the gram-negative bacterium *Stigmatella aurantiaca* (Myxobacteria)[1] is covalently attached by a phosphate ester linkage to an RNA (branched-RNA) This branched RNA consists of a triribonucleotide, [5] A-G-C/U[3] , which branches out from the 2'-position at the G residue, forming a 2'→ 5' phosphodiester linkage with the 5'-end of dC residue of the msDNA The branched RNA part consists of stem-and-loop structures, while the msDNA part is double-stranded The 3'-end parts of both branched RNA and msDNA constitute the RNA-DNA hybrid structure This form of mature branched RNA-msDNA molecule appears to be very stable in cells, which seems to play an important role during the life cycle of myxobacteria. The resemblance of the core branched RNA-msDNA structure **13** to the lariat RNAs that are intermediates in RNA splicing[19,24] has prompted us to devise its synthesis and its RNA counterpart **14** We subsequently report our assessment of their solution structures by a comparative conformational study on this unique branched RNA-DNA conjugate **13** and its RNA counterpart **14**

Chemistry. Since we wished to understand the differences in the conformational features between a branched DNA-RNA conjugate **13** and a corresponding branched RNA **14** by high field NMR spectroscopy, we were interested to develop synthetic strategy which would produce *large amount* (~40 mg) of the *pure* branched oligonucleotide Clearly, an unambiguous synthetic route meeting this demand requires that all phosphate ester

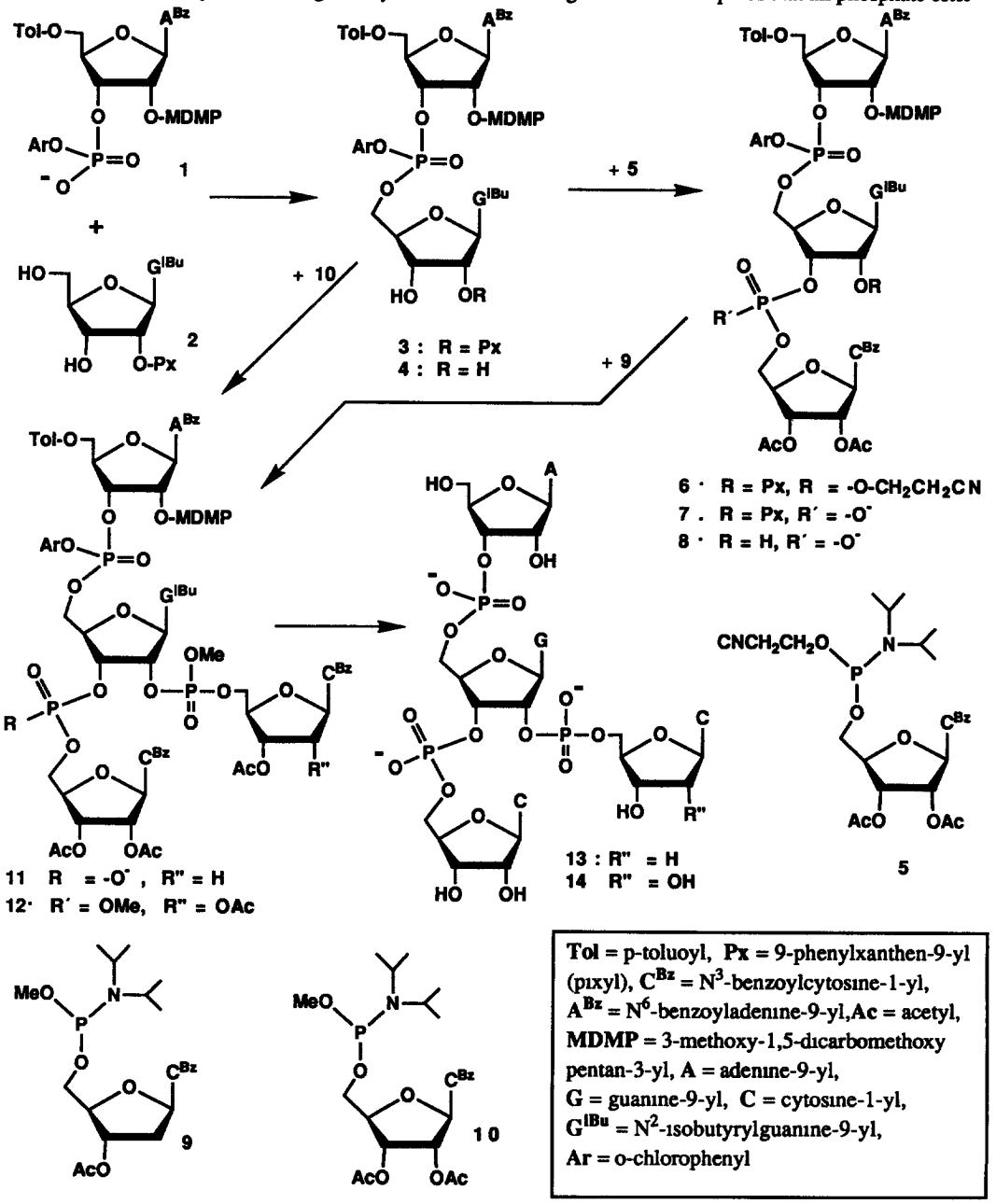

Tol = p-toluoyl, **Px** = 9-phenylxanthen-9-yl (pixyl), C^{Bz} = N^3-benzoylcytosine-1-yl, A^{Bz} = N^6-benzoyladenine-9-yl, **Ac** = acetyl, **MDMP** = 3-methoxy-1,5-dicarbomethoxy pentan-3-yl, **A** = adenine-9-yl, **G** = guanine-9-yl, **C** = cytosine-1-yl, G^{IBu} = N^2-isobutyrylguanine-9-yl, **Ar** = o-chlorophenyl

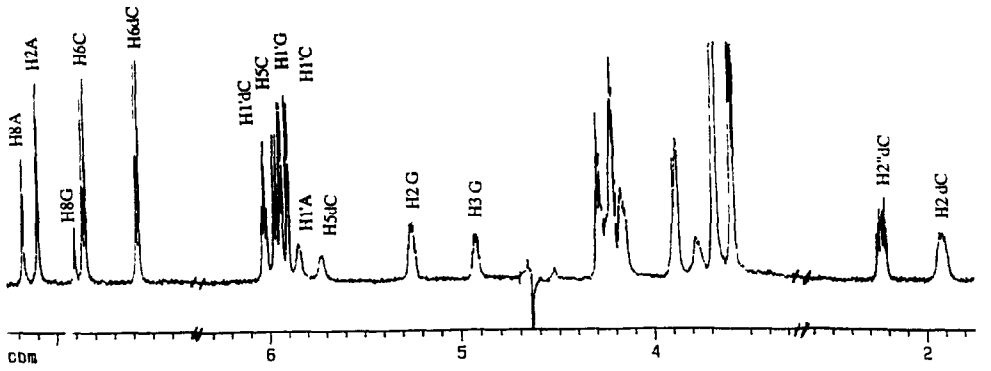

Fig 1 1D spectrum of A3´p5´G$^{2'p5'dC}_{3'p5'C}$ (**13**) at 35 °C and at concentration 1.8 mM

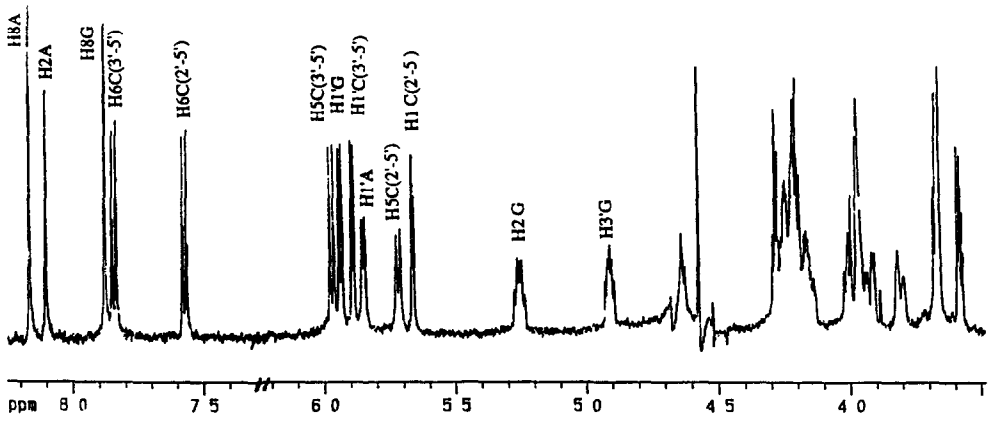

Fig. 2 1D spectrum of A3´p5´G$^{2'p5'C}_{3'p5'C}$ (**14**) at 35 °C and at concentration 1 8 mM

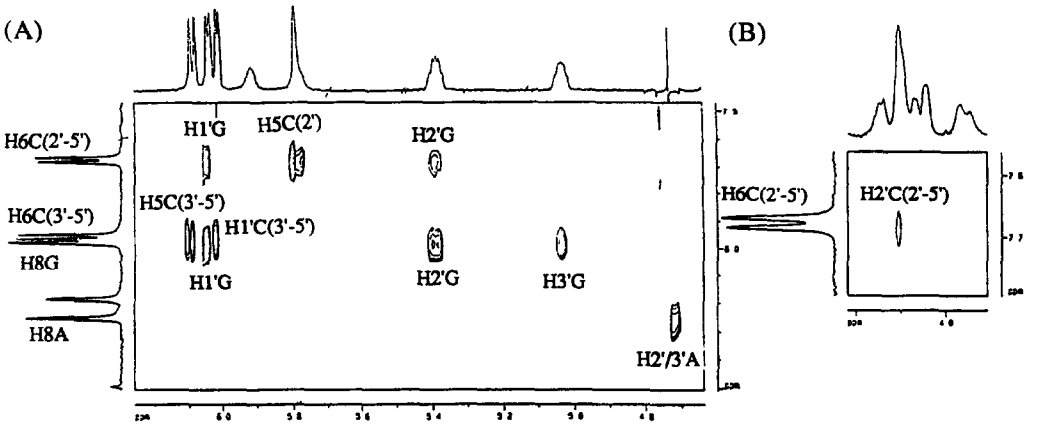

Fig 12 ROESY spectrum of **14** at 30 °C (1.8 mM)
(A) and(B) are zooms taken of different parts of the spectrum.

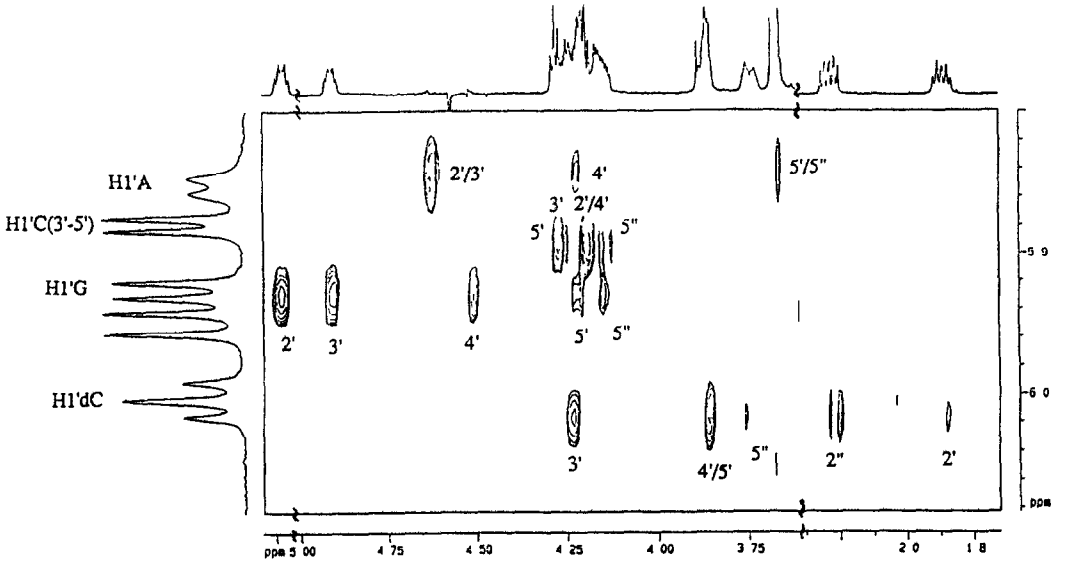

Fig. 3 HOHAHA spectrum of A3′p5′G$^{2'p5'dC}_{3'p5'C}$ (**13**) at 35 °C and at concentration 1 8 mM

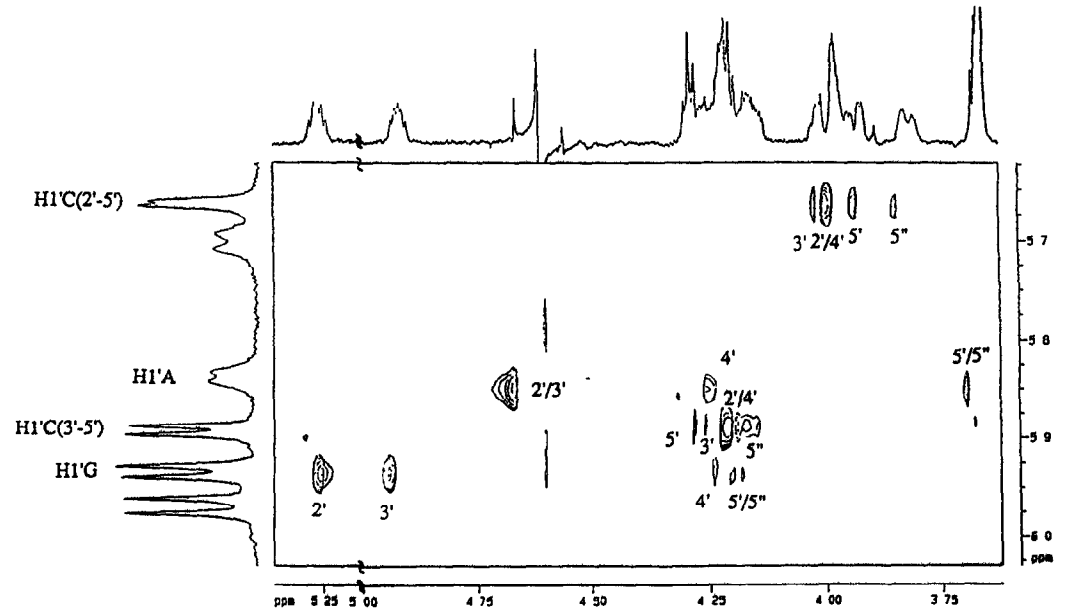

Fig 4 HOHAHA spectrum of A3′p5′G$^{2'p5'C}_{3'p5'C}$ (**14**) at 35 °C and at concentration 1 8 mM

groups are regiospecifically introduced This is particularly important in reactions which involve the sequential phosphorylation of the vicinal 2′- and 3′-hydroxyl groups of the branch-point nucleoside. Earlier studies have shown that there are only two successful ways to introduce the second phosphate ester function regiospecifically vicinal to a 2′- or 3′-phosphate of a *cis*-diol system as in the branch-point ribonucleoside· (1) introduction of a S,S-diphenylphosphorodithioate at 2′-OH in N^6-benzoyladenosine-3′-phosphorodianilidate in the presence of mesitylenedisulfonyl chloride[2], and (2) introduction of the second 2′→5′ or 3′→5′ phosphate ester group vicinal to a *phosphodiester* fuction by either phosphoroamidite[3] or H-phosphonate[4] methodologies. A survey of synthetic methods[3a,e,h] devised for the preparation of tetrameric branched RNA reveals that the shortest route to their synthesis involves the condensation of an appropriately protected 5′-H-phosphonate ester of a nucleoside[3h] with a dimer such as **3** This allows the introduction of the vital *diester* linkage directly at the vicinal diol of the branch-point of the resultant trinucleotide in one step However, during the development of this method[3h], we observed the loss of the acid-labile 2′-O-(9-phenylxanthen-9-yl) group during oxidation/work-up of the reaction mixture although the consequence of such loss was quite harmless In the present work, we decided to use a sequential phosphorylation for the synthesis of the core tetramer of the RNA-DNA conjugate **13** and its RNA counterpart **14** Appropriately protected 3′→5′ phosphotriester linked dimer **3** was first prepared in 75 % yield by the regioselective condensation of N^6-benzoyl-5′-O-(4-toluoyl)-2′-O-(3-methoxy-1,5-dicarbomethoxypentan-3-yl (MDMP)[5]-3′-O(2-chlorphenyl)phosphodiester (**1**) with N^2-isobutyryl-2′-O-(9-phenylxanthen-9-yl) (**2**)[6] in the presence of 1-mesitylenesulfonyl-3-nitro-1,2,4-triazole (MSNT)[7] using the phosphotriester methodology[8] One part of this dimer was coupled with the β-cyanoethylphosphoroamidite[9] block **5** by standard phosphoroamidite chemistry[10] giving the desired fully protected trimer **6** (79 %) Treatment of this trimer with dry triethylamine[11] in dry pyridine for 11 h provided the desired diester linkage with the intact vicinal 2′-O-pixyl group[12] in the partially-protected trimer block **7** (89 %) Partially-protected trimer block **7** was then treated with a solution of 0 05 M trichloroacetic acid in 2 % ethanol-chloroform (v/v) at 0 °C for 20 min for the regioselective removal of the 2′-O-pixyl group in the presence of the acid-labile 2′-O-MDMP[5] group giving the 2′-hydroxy trimer block **8** in 74 % yield It should be noted that the success of this selective acidic removal of the 2′-O-pixyl group in the presence of the acid-labile 2′-O-MDMP group in **7** to give **8** is a consequence of the stabilization of the 2′-O-MDMP group exerted by the vicinal 3′→5′ phosphotriester linkage[13] versus the vicinal phosphodiester group promoted lability[14] of the 2′-O-pixyl group Subsequent coupling of **8** with phosphoroamidite **9** in the presence of 1,2,3,4-tetrazole, oxidation by iodine in pyridine-THF-water[10] followed by purification by short column chromatography afforded the desired partially protected molecule **11** in 76 % yield Deprotection of this tetramer (see experimental) and purification on DEAE-Sephadex A-25 column gave 709 A_{260} o d units of the pure RNA-DNA conjugate **13** (33 %) The RNA counterpart **14**, which is symmetrically linked both at 2′→5′ and 3′→5′ directions, was synthesized in the following manner the dimer **3** was treated with 0 05 M trichloroacetic acid in 2 % ethanol-chloroform (v/v) at 0 °C for 8 h for the regioselective removal of the 2′-O-pixyl group in the presence of the acid-labile 2′-O-MDMP[5] group giving the 2′,3′-dihydroxy dimer block **4** in 58 % yield The dimer **4** was subsequently coupled with a large excess (7 equiv) of the phosphoroamidite block **10** by standard phosphoroamidite methodology[10] giving the fully protected symmetrically 2′→5′ and 3′→5′ linked tetramer **12** in 84 % yield Subsequent deprotection (see experimental) and anion excange chromatography gave 976 A_{260} o d units of the tetramer **14** (38 %)

*Assignment of ^1H and ^{31}P resonances in branched tetramers **13** & **14**.* All the sugar protons and non exchangeable base protons in tetramers **13** and **14** could be assigned from the interpretation of several 2D NMR

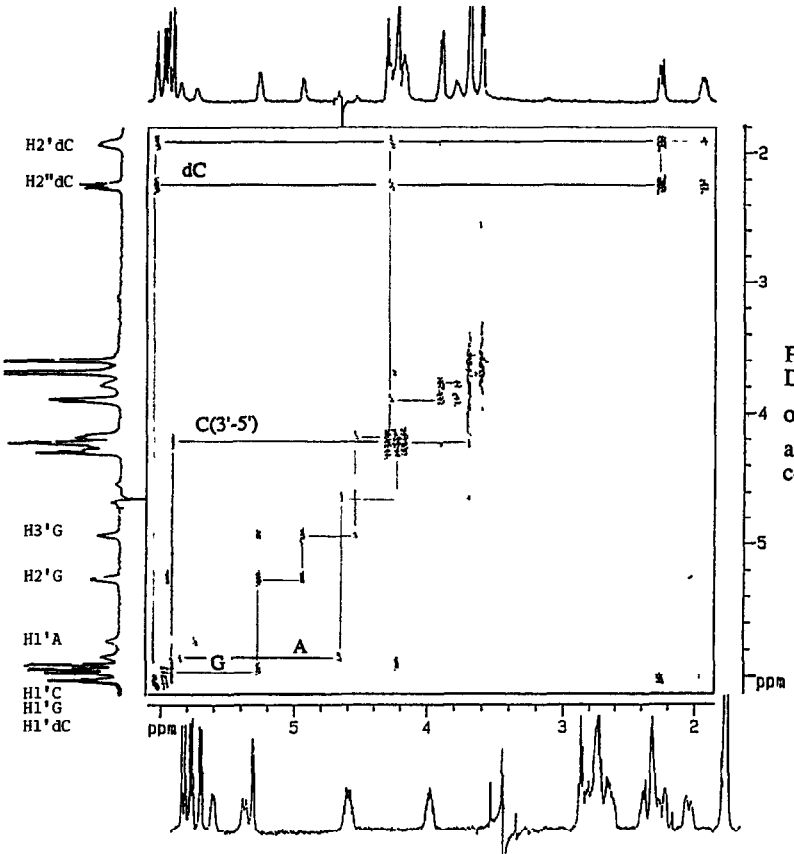

Fig 5
DQF-COSY spectrum of A3′p5′G$^{2'p5'dC}_{3'p5'C}$ (**13**) at 30°C and at concentration 1 8 mM

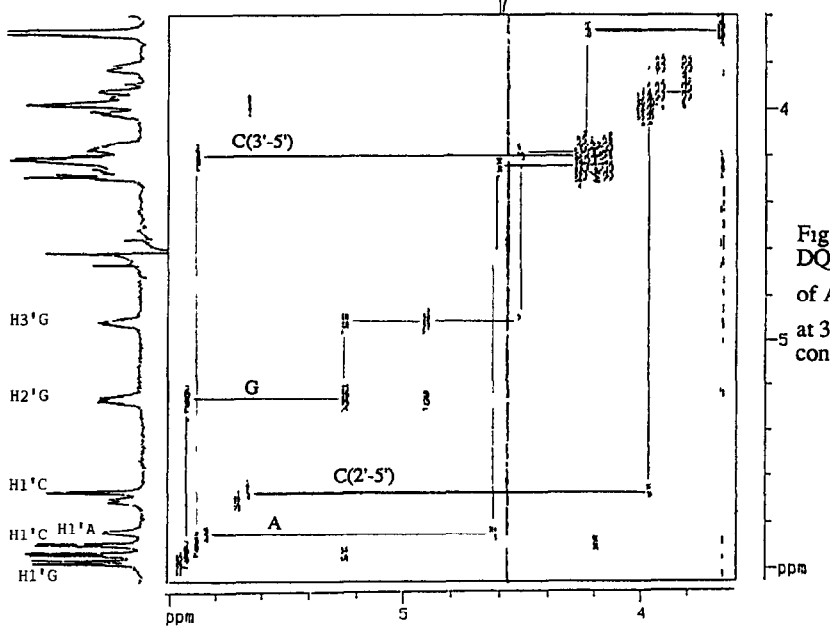

Fig 6
DQF-COSY spectrum of A3′p5′G$^{2'p5'C}_{3'p5'C}$ (**14**) at 30°C and at concentration 1 8 mM

spectra such as HOHAHA[15] (Figures 3 & 4), DQF-COSY[16] (Figures 5 & 6), 2D ^{1}H-^{31}P[26] correlation (Figures 7 & 8) and NOESY (Figures 9 & 10) and ROESY[25] (Figures 11 & 12) The branch-point guanosine residue in both tetramers was easily assigned due to the downfield shift of its H2' and H3' protons because of the presence of electron-withdrawing 2′→ 5′ and 3′→ 5′ phosphodiester residues The 5'-terminal adenosine residue in both tetramers was identified by the upfield shift of its H5'/H5" protons and the downfield shift of its H3' proton The two remaining sugars in tetramer **13** were differentiated by the different shifts of the cross peaks of H2' and H2" protons of deoxycytidine in the HOHAHA spectrum (Fig 3) In tetramer **14** the two remaining cytidine residues were identified by the interpretation of a 2D ^{1}H-^{31}P correlation spectrum (Fig 8) The 2′→ 5′ phosphate is always the most shielded ^{31}P signal and it experiences a spin-spin coupling with the H5'/H5" of the 2'-cytidine and H2' of guanosine The non exchangeable base protons in both tetramers were assigned with the help of NOESY and ROESY spectra

Table 1 Chemical shifts of branched RNA-DNA conjugate **13**

	Temp	H1'	H2'	H2"	H3'	H4'	H5'	H5"	H8	H2	H6	H5
Ap	30°C	5 84	4 64	-	4 64	4 23	3 68	3 68	8 17	8 09	-	-
	60°C	5 90	4 66	-	4 64	4 37	3 66	3 66	8 18	8 14	-	-
pGp	30°C	5 92	5 25	-	4 92	4 52	4 23	4 16	7 89	-	-	-
	60°C	5 94	5 23	-	4 90	4 52	4 25	4 15	7 91	-	-	-
pdC[2'→5']	30°C	6 01	1 90	2 22	4 25	3 87	3 77	3 77	-	-	7 56	5 72
	60°C	6 02	1 91	2 23	4 27	4 21	3 86	3 86	-	-	7 58	5 80
pC[3'→5']	30°C	5 89	4 20	-	4 29	4 20	4 16	4 14	-	-	7 84	5 95
	60°C	5 88	4 19	-	4 20	4 19	4 12	4 12	-	-	7 82	5 96

Table 2 Chemical shifts of **14**

	Temp	H1'	H2'	H3'	H4'	H5'	H5"	H8	H2	H6	H5
Ap	30°C	5 83	4 63	4 63	4 22	3 64	3 64	8 16	8 09	-	-
	60°C	5 89	4 65	4 64	4 25	3 66	3 66	8 17	8 14	-	-
pGp	30°C	5 93	5 26	4 91	4 52	4 23	4 17	7 88	-	-	-
	60°C	5 95	5 24	4 90	4 51	4 22	4 17	7 89	-	-	-
pC[2'→5']	30°C	5 67	3 97	4 00	3 95	3 92	3 81	-	-	7 57	5 69
	60°C	5 69	3 96	4 01	3 97	3 91	3 80	-	-	7 59	5 97
pC[3'→5']	30°C	5 89	4 20	4 23	4 22	4 26	4 15	-	-	7 85	5 97
	60°C	5 88	4 18	4 22	4 21	4 23	4 14	-	-	7 83	5 97

Conformational analysis of branched tetramers 13 & 14. The proton and phosphorus chemical shifts of both tetramers were measured at different temperatures (25 - 80 °C) at concentrations of 1 8 mM and 6 4 mM for **13**, and 0 7 mM, 1 8 mM, 6 4 mM and 11.9 mM for **14** because the chemical shifts of both aromatic and sugar protons were highly concentration- and temperature-dependent Owing to these reasons, we also obtained the ^{1}H-^{1}H and ^{1}H-^{31}P coupling constants of tetramers **13** and **14** at two different temperatures (30 and 60 °C) from DQF-COSY[16] and E-COSY[17] experiments with and without phosphorus decoupling. E-COSY spectra have shown definite advantages in delineating the coupling constants in the crowded H5'/H5" region which in DQF-COSY spectrum shows only complex overlap (Fig 18)

(A) Temperature-dependence of chemical shifts The δ-values of the non-exchangeable base protons and the anomeric protons are highly sensitive to ring current effects exerted by spatialy proximate bases Therefore, the temperature-dependent aromatic and anomeric chemical shifts provide a suitable probe to observe stacking phenomena in oligonucleotides. In particular, protons residing above or below the plane of a purine base experience considerable shielding These protons are expected to show large Δδ values upon increasing the

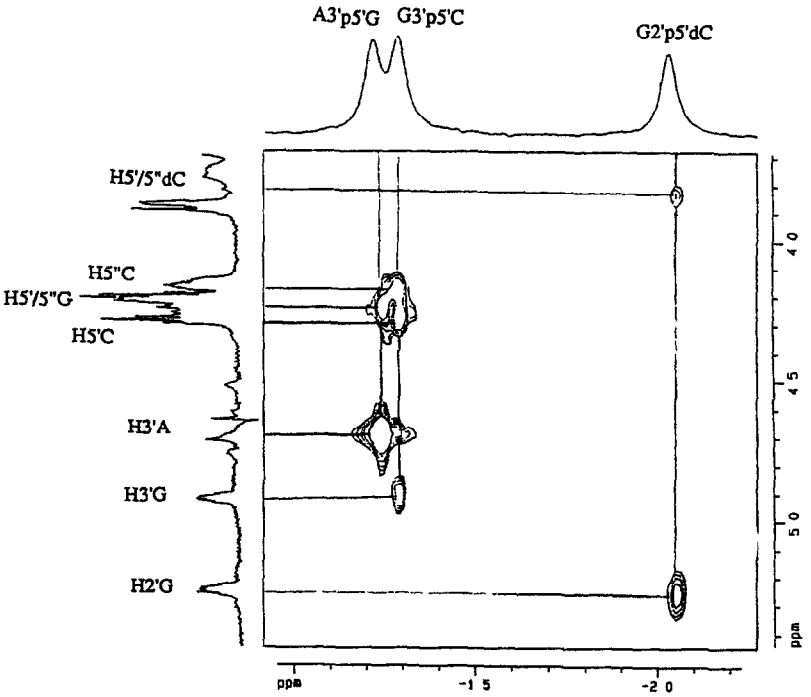

Fig. 7 ^{1}H-^{31}P correlation spectrum of A3´p5´G$^{2'p5'dC}_{3'p5'C}$ (13) at 35 °C and at concentration 1 8 mM

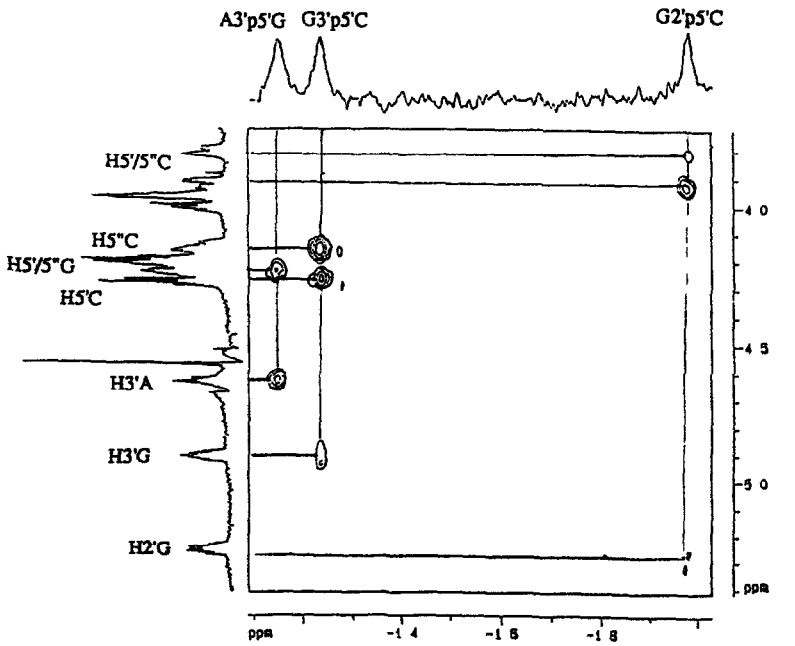

Fig. 8 ^{1}H-^{31}P correlation spectrum of A3´p5´G$^{2'p5'C}_{3'p5'C}$ (14) at 35 °C and at concentration 1.8 mM

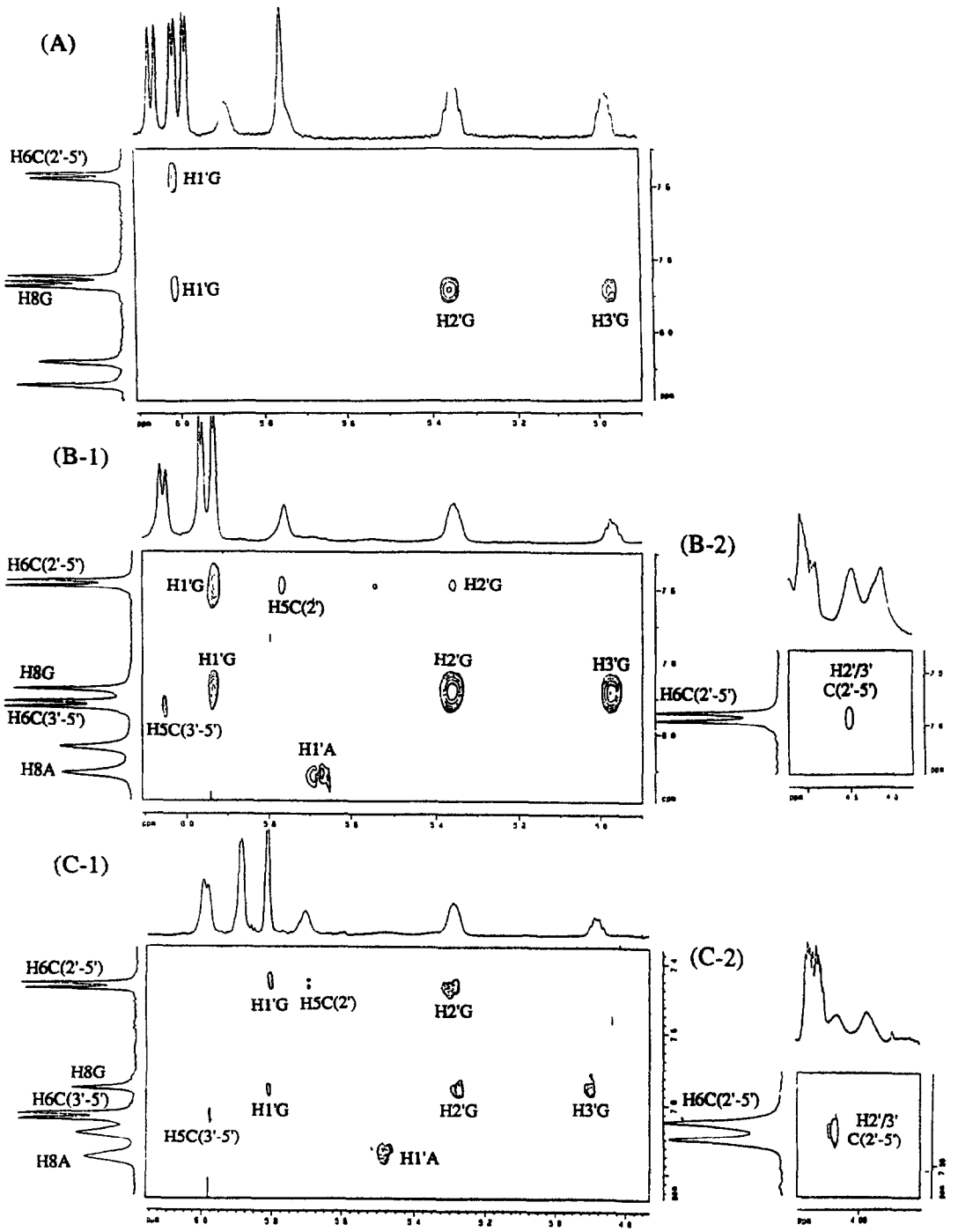

Fig 10 NOESY spectra of 14 at 30 °C (A) at 1 8 mM (B-1), (B-2) at 6 4 mM, (C-1) and (C-2) at 11 9 mM

temperature, with gradual disruption of the stacking interactions. Especially H2A and H5C/dC are good markers for detection of base-base stacking interaction, interpretation of Δδ for H6C/dC, H8A and H8G is more difficult, since the chemical shifts of these protons also depend on the conformation around the glycosidic bond[18] The temperature dependent studies of both tetramers have been made at 1.8 mM concentration. The Δδ for all non-exchangeable base protons and anomeric protons for both tetramers are given in Table 5. Figures 13 and 14

Table 4. Coupling constants of **14** obtained from DQF-COSY at 500 MHz*

	Temp	$J_{1',2'}$	$J_{2',3'}$	$J_{3',4'}$	$J_{4',5'}$	$J_{4',5''}$	$J_{5',5''}$	$J_{2',P2'}$	$J_{3',P3'}$	$J_{4',P5'}$	$J_{5',P5}$	$J_{5'',P5''}$
Ap	30 °C	5 4	5 8	3 4	5 8		a	-	6 1	-	-	-
	60 °C	5 6	5 6	3 6	6 1		a	-	6 1	-	-	-
pGp	30 °C	5 3	5 0	4 0	7 9		9 4	9 3	7 9	a	9 1	
	60 °C	5 9	5 3	3 9	2 6	5 7	11 6	8 6	7 1	a	4 6	4 1
pC2´p	30 °C	2 1	5 5	6 7	2 1	1 8	11 4	-	-	-	4 1	2 0
	60 °C	3 1	5 0	6 7	2 8	2 8	11 4	-	-	-	5 2	4 9
pC3´p	30 °C	4 3	5 4	a	2 3	3 4	11 9	-	-	-	4 2	6 1
	60 °C	4 3	4 9	a	2 5	3 5	11 8	-	-	-	5 6	5 0

* resolution 1 Hz/point, (a) could not be determined

Table 5 δ- and Δδ-values at 25 & 80°C for the aromatic and the anomeric protons of **13** and **14**

		H2			H8			H6			H5			H1'		
	Residues	25°C	80°C	Δδ*	25°C	80°C	Δδ	25°C	80°C	Δδ	25°C	80°C	Δδ	25°C	80°C	Δδ
13	A	8 066	8 158	0 092	8 152	8 175	0 023	-	-	-	-	-	-	5 807	5 909	0 102
	G	-	-	-	7 885	7 909	0 024	-	-	-	-	-	-	5 918	5 958	0 04
	dC[2'→5']	-	-	-	-	-	-	7 561	7 594	0 033	5 683	5 834	0 151	6 019	6 036	0 017
	C[3'→5']	-	-	-	-	-	-	7 847	7 814	0 033	5 958	5 968	0 01	5 896	5 884	0 012
14	A	8 069	8 159	0 09	8 145	8 171	0 026	-	-	-	-	-	-	5 798	5 904	0 106
	G	-	-	-	7 869	7 894	0 025	-	-	-	-	-	-	5 926	5 960	0 034
	C[2'→5']	-	-	-	-	-	-	7 568	7 600	0 032	5.673	5 812	0 139	5 673	5 719	0 046
	C[3'→5']	-	-	-	-	-	-	7 862	7 822	0 04	5.980	5 980	0	5 902	5 884	0 018

*Δδ = δH at 80°C - δH at 25°C

show the δ vs temperature profiles for tetramers **13** and **14**, respectively Both tetramers showed an almost identical behaviour upon increase in temperature (25 - 80 °C) Among the base protons, we could observe a large downfield shift of H2A (Δδ = 0 09 ppm for both **13** and **14**) and H5 of the 2´→ 5´ linked residue (Δδ = 0 151 ppm for dC in **13** & 0 139 ppm for C in **14**) indicating that these two residues are part of the stacked geometry The large Δδ of H2A could be explained by the ring current of the branch-point G, the downfield shift of the H8G suggests (Δδ = 0 024 ppm for **13**, 0 025 ppm for **14**) that G is also stacked in both tetramers Note that in the naturally-occurring branched triribonucleotide $A^{2'p5'G}_{3'p5'U}$ the H8G has a Δδ of 0 042 ppm

Table 6 Phosphorus chemical shifts (at 10 °C and 80 °C) and Δδ-values for **13** and **14**

	A3´p5´$G^{2'p5'dC}_{3'p5'C}$ (**13**)			A3´p5´$G^{2'p5'C}_{3'p5'C}$ (**14**)		
Temperature	A3'p5'G	G2'p5'dC	G3'p5'C	A3'p5'G	G2'p5'C	G3'p5'C
10°C	-1 837	-2 640	-1 550	-1 668	-2 713	-1 668
80°C	-0 641	-1 230	-0 901	-0 688	-1 451	-0 895
Δδ	1 196	1 41	0 649	0 98	1 262	0 773

Δδ = δ^{31}P at 80°C - δ^{31}P at 10°C

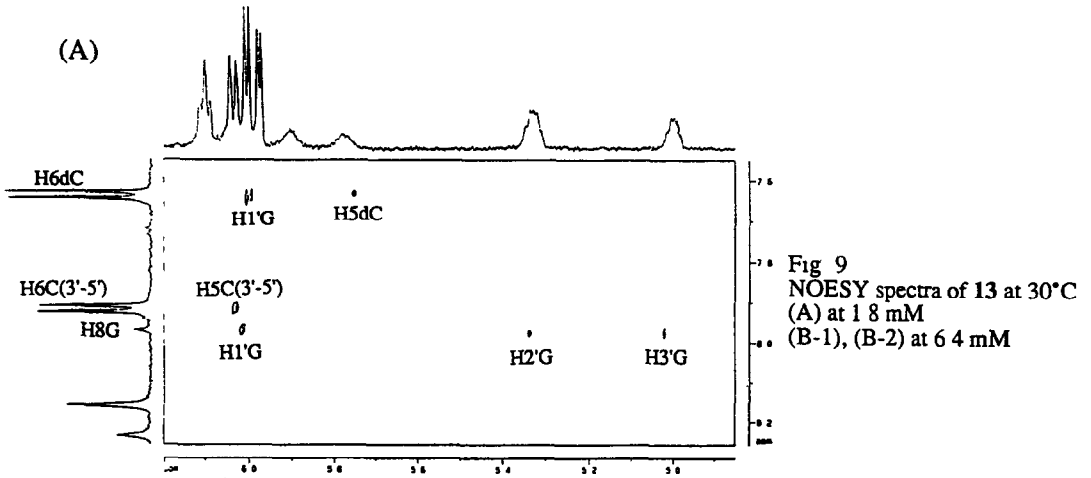

Fig 9
NOESY spectra of 13 at 30°C
(A) at 1 8 mM
(B-1), (B-2) at 6 4 mM

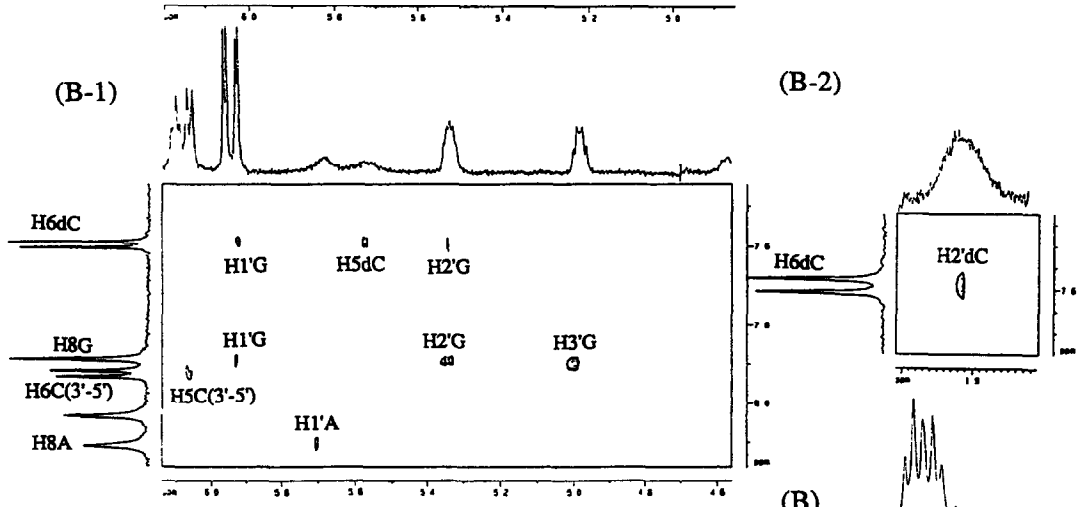

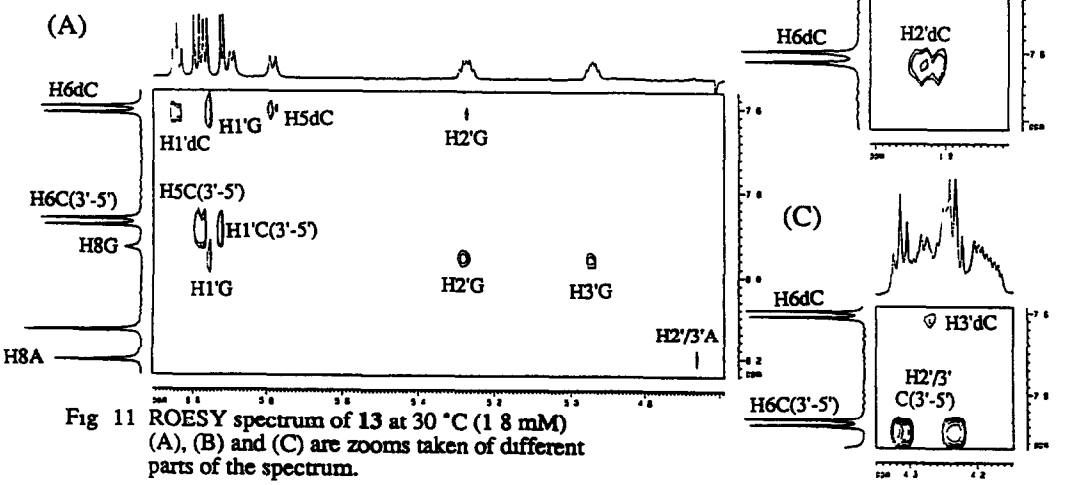

Fig 11 ROESY spectrum of 13 at 30 °C (1 8 mM)
(A), (B) and (C) are zooms taken of different parts of the spectrum.

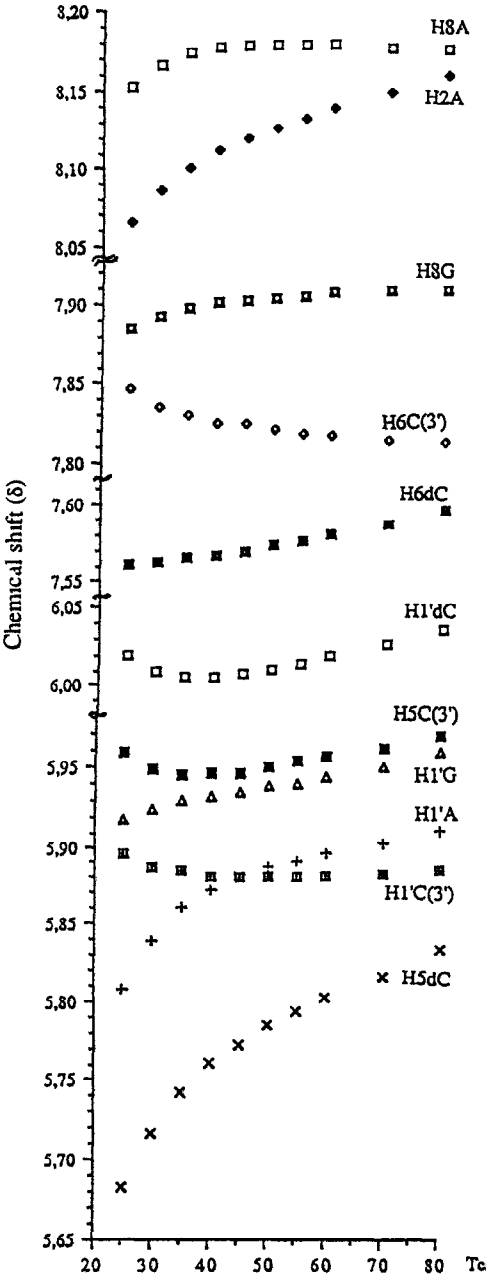

Fig. 13 Plot of ^{1}H chemical shift vs temperature for A3´p5´G$^{2'p5'dC}_{3'p5'C}$ (13) at concentration 1.8 mM

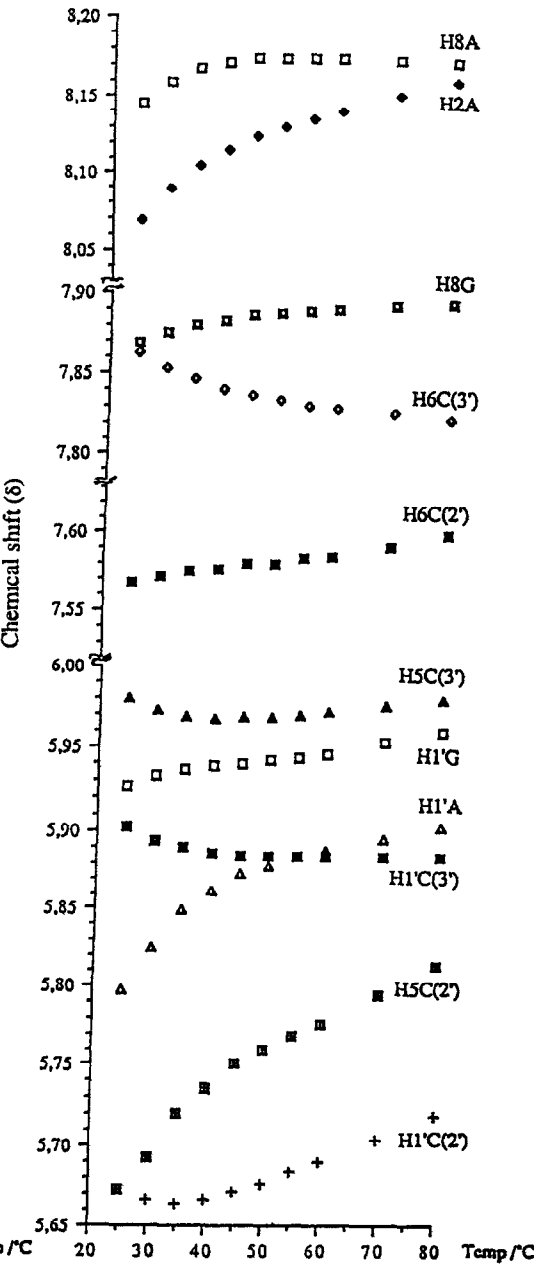

Fig. 14 Plot of ^{1}H chemical shift vs temperature for A3´p5´G$^{2'p5'C}_{3'p5'C}$ (14) at concentration 1 8 mM

which has been implicated as the moderately flexible 2′→ 5′ stacked state between A and G residues[19] The stacking along A3'→ 5'G2'→ 5'dC in **13** or A3'→ 5'G2'→ 5'C in **14** is also supported by the fact that the H1'A (Δδ = 0 102 ppm for **13**, 0.106 ppm for **14**), H1'G (Δδ = 0 04 ppm for **13**, 0 034 ppm for **14**) and the H1' of the 2′→ 5′ linked residue (Δδ = 0.017 ppm for **13** (dC), 0 046 ppm for **14** (C)) undergo a clear downfield shift upon increase of temperature from 25 - 80 °C Looking at the temperature-dependent phosphorus chemical shifts (Table 6, Fig. 15) we find that the A3'p5'G (Δδ = 1 196 ppm) and G2'p5'dC (Δδ = 1 41 ppm) moieties in **13** or A3'p5'G (Δδ = 0.98 ppm) and G2'p5'C (Δδ = 1 262 ppm) moieties in **14** show the largest shift upon increasing the temperature from 10 to 80 °C , which again supports the A3'→ 5'G2'→ 5'dC (or C) stacking in these branched tetramers Foregoing comparison of the Δδ-values for the aromatic and anomeric protons and for phosphorus in the two tetramers showed that the branched tetramer **13** is clearly more affected upon an increase in the temperature than the tetramer **14**, suggesting that the former has distinctly more pronounced intramolecularly stacked structure than the latter. Further characteristic evidence for G2'→ 5'dC stacking in **13** or G2'→ 5'C stacking in **14** came from our NOESY and ROESY experiments at 900 ms (at 1 8 mM and 6 4 mM concentrations) which showed NOE or ROE cross peaks between H6C(or dC) and H1'G and H2'G (Figs. 9, 10 and 11, 12)

(B) Concentration dependence of chemical shifts A study of the concentration dependence of chemical shifts was carried out on tetramer **13** (1 8 mM and 6 4 mM) and **14** (0.7 mM, 1 8 mM, 6.4 mM and 11 9 mM) The Δδ for all non-exchangeable base protons and anomeric protons for both tetramers are given in Tables 7 and 8 Figures 16 and 17 show the δ vs concentration for both tetramers Again both tetramers showed an almost identical behaviour We could observe an upfield shift of H2A (Δδ = 0 033 ppm for **13**, Δδ = 0 085 ppm for **14**), the H5 of the 2'→ 5' linked residue (Δδ = 0.075 ppm for **13**, Δδ = 0 285 ppm for **14**) and the H1'A (Δδ = 0 09 ppm for **13**, Δδ = 0 228 ppm for **14**), indicating an increased shielding of 5′-terminal adenosine and the 2'→ 5' linked terminal C or dC residue upon an increase of the concentration At the same time the chemical shifts of H8 and H1' of guanosine show only small changes (Δδ = 0 03 ppm for H8 and 0 01 ppm for H1' in **13**, Δδ = 0 007 ppm for H8 and 0 016 ppm for H1' in **14**) and the H5 and H1' of the 3'→ 5' linked cytosine are shifted downfield (Δδ = 0 05 ppm for H5 and 0 02 ppm for H1' in **13**, Δδ = 0 123 ppm for H5 and 0 088 ppm for H1'in **14**) so is the H1' of the 2'→ 5' linked residue (Δδ = 0.01 ppm for **13**, Δδ = 0 145 ppm for **14**) A logical explanation for this behaviour is that upon the concentration increase the tetramers start to aggregate by stacking on top of each other in a vertical manner, meaning that the 2'→ 5' linked residue (dC or C) of one molecule of the branched tetramer stacks vertically on top of the 5'-terminal adenosine of a second molecule of the branched tetramer, while at the same time retaining an intramolecular conformation which is closely similar to the ones found at the monomeric state at a diluted concentration (1.8 mM) This vertically stacked geometry of the aggregate state due to intermolecular association clearly explains why the chemical shifts of the core branch-

Table 7 Chemical shifts and Δδ-values* of **13** at different concentrations at 35 °C

	H2			H8			H6			H5			H1'		
residue	1 8M	6 4M	Δδ	1 8M	6 4M	Δδ	1 8M	6 4M	Δδ	1 8M	6 4M	Δδ	1.8M	6 4M	Δδ
A	8 100	8 067	0 033	8 170	8 120	0 05	-	-	-	-	-	-	5 860	5 770	0 09
G	-	-	-	7 900	7 870	0 03	-	-	-	-	-	-	5.930	5 920	0 01
dC[2'→5']	-	-	-	-	-	-	7 560	7 570	0 01	5 740	5 665	0 075	6 005	6 015	0 01
C[3'→5']	-	-	-	-	-	-	7 830	7 840	0 01	5 950	6 000	0 05	5 880	5.900	0.02

*Δδ difference in chemical shift at 1.8 mM and 6 4 mM

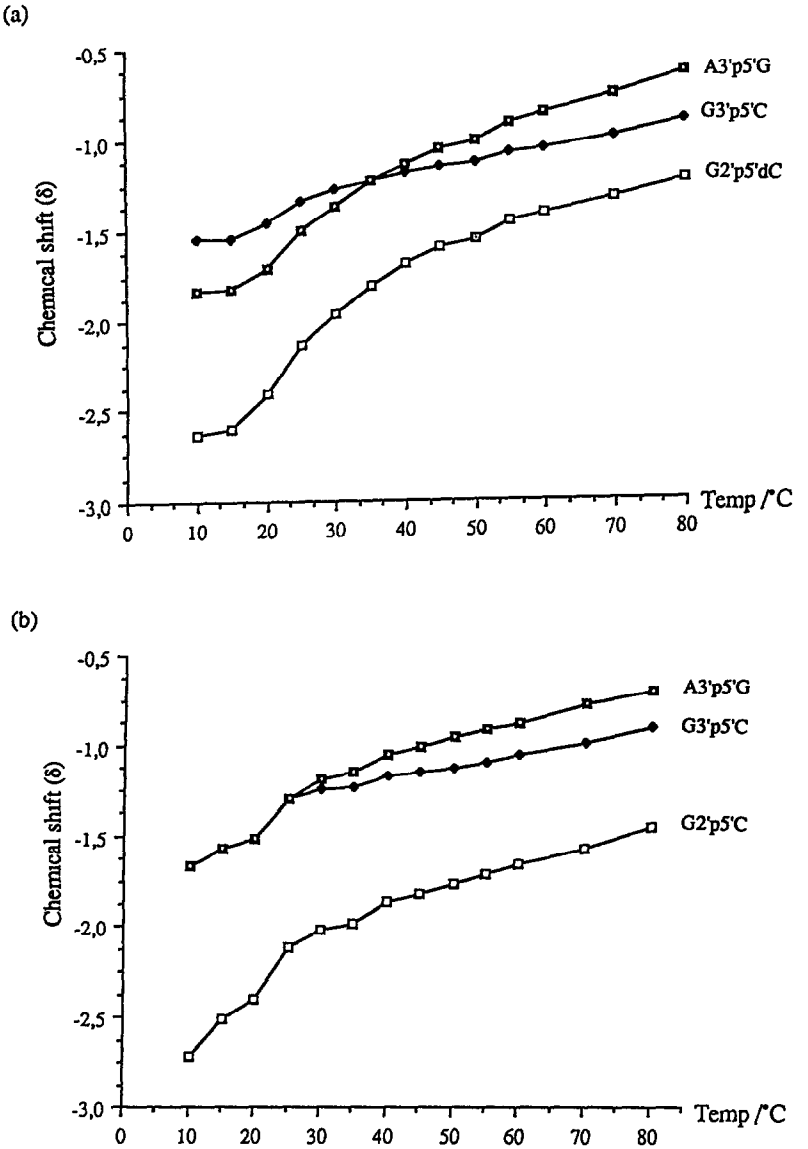

Fig 15 Plot of ^{31}P chemical shift vs.temperature at concentration 1.8 mM for (a) A3´p5´$G^{2'p5'dC}_{3'p5'C}$ (**13**) (b) A3´p5´$G^{2'p5'C}_{3'p5'C}$ (**14**)

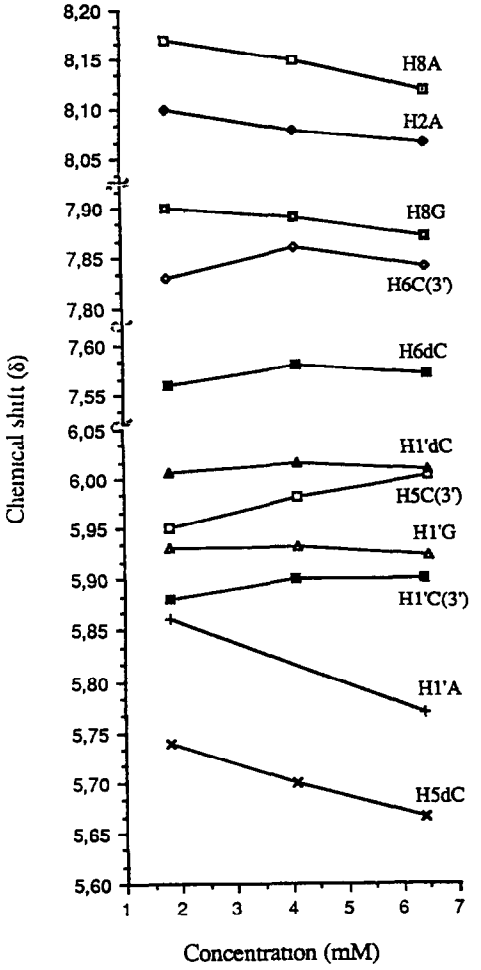

Fig 16 Plot of 1H chemical shift vs concentration for A3´p5´$G^{2'p5'dC}_{3'p5'C}$ (**13**) at 30°C

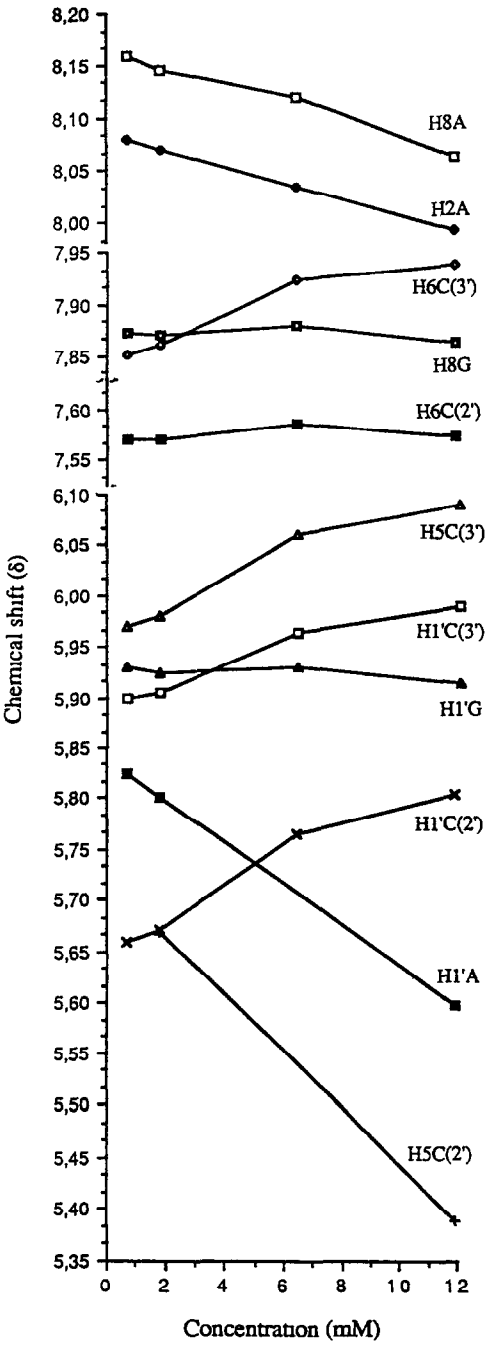

Fig. 17 Plot of 1H chemical shift vs concentration for A3´p5´$G^{2'p5'C}_{3'p5'C}$ (**14**) at 30°C

point guanosine remain almost unaffected upon an increase in concentration while at the same time the adenosine and the 2'→ 5' linked dC or C residue show considerable shielding

(C) Conformation of the sugar ring In aqueous solution, the sugar ring of a ribonucleotide or a deoxyribonucleotide is known to exist in an equilibrium of two rapidly interconverting conformers denoted by North (C2'-*exo* and C3'-*endo*) and South (C2'-*endo*, C3'-*exo*) The geometries of the North (N) and South (S) conformers are expressed as their phase angles of pseudorotation ($P_N = 0° \leq 36°$ and $P_S = 144° \leq 190°$) and their puckering amplitudes (ϕ_N and ϕ_S) are generally around 36 - 40° The molar fractions of the N and S pseudorotamer population can be deduced from the ^1H-^1H coupling constants[27] $J_{1'2'}$, $J_{2'3'}$ and $J_{3'4'}$ for ribo- and $J_{1'2'}$, $J_{1'2''}$, $J_{2'3'}$, $J_{2''3'}$, $J_{3'4'}$ for deoxyribonucleotide using the program PSEUROT[20] In RNA and DNA a full

Table 8· Chemical shifts and Δδ-values* of **14** at different concentrations at 25 °C

	H2			H8			H6			H5			H1'		
residue	0 7M	11 9M	Δδ	0 7M	11 9M	Δδ	0 7M	11 9M	Δδ	0 7M	11 9M	Δδ	0 7M	11 9M	Δδ
A	8 080	7 995	0 085	8 160	8 067	0 093	-	-	-	-	-	-	5 825	5 597	0 228
G	-	-	-	7 873	7 866	0 007	-	-	-	-	-	-	5 930	5 914	0 016
C[2'→5']	-	-	-	-	-	-	7 570	7 576	0 006	5 670#	5 385	0 285	5 662	5 807	0 145
C[3'→5']	-	-	-	-	-	-	7 853	7 943	0 090	5 970	6 093	0 123	5 900	5 988	0 088

1 8 mM concentration, *Δδ difference of chemical shifts at 0 7 mM and 11 9 mM

pseudorotational analysis requires the measurement of the coupling constants at different temperatures but the overlap of sugar proton absorptions often makes an accurate determination of all coupling constants difficult It is however, possible to estimate the population of N type conformer from the $J_{1'2'}$ coupling constant for RNA and from the $J_{1'2'}$ and $J_{1'2''}$ coupling constants for DNA using the equations 1 & 2[21]

$$\%N = 100((7\,9 - J_{1'2'})/6\,9) \quad (1)$$

$$\%N = 100(1 - ((J_{1'2'}+J_{1'2''}-9\,8)/5\,9)) \quad (2)$$

The pseudorotational parameters for **13** and **14** were calculated using the program PSEUROT [20] and are listed in Table 9 Both tetramers exhibit similar behaviour, the sugars of adenosine and guanosine seem to be oriented toward the S conformation (~75% S for both adenosines and ~66% S for both guanosines), the 3'→5'linked cytidine of both **13** and **14** does not show any preference for the N or S type conformation Upon increase in temperature neither of these sugars seems to be affected to any great extent The sugar of the 2'→ 5' linked cytidine in tetramer **14** prefers the N conformation and the increase in temperature results in a decrease of the polulation of the N conformer In tetramer **13** the 2'→ 5' sugar of deoxycytidine does not show any preference for the N or S conformation and is not to any great extent affected by any increase in temperature

Table 9 Pseudorotational parameters P, ϕ and population of N type conformer (%) from PSEUROT progam

	$A3'p5'G^{2'p5'dC}_{3'p5'C}$ (**13**)				$A3'p5'G^{2'p5'C}_{3'p5'C}$ (**14**)			
	Ap	pGp	pdC[2'→5']	pC[3'→5']	Ap	pGp	pC[2'→5']	pC[3'→5']
P_N	2°	12°	-4°	a	18°	7°	-5°	a
ϕ_N	38°	35°	40°	a	36°	39°	35°	a
P_S	158°	162°	171°	a	154°	150°	137°	a
ϕ_S	35°	36°	41°	a	35°	38°	39°	a
%N at 30°C	24	34	53	a (54)*	28	34	81	a (52)*
%N at 60°C	21	27	48	a (52)*	28	29	73	a (52)*

(a) could not be determined, * calculated using formula $\%N = 100((7\,9 - J_{1'2'})/6\,9)$

Table 3 Coupling constants of A3′p5′$G^{2'p5'(dC)}_{3'p5'C}$ (13) obtained from DQF-COSY at 500 MHz*

	Temp	$J_{1',2'}$	$J_{1',2''}$	$J_{2',2''}$	$J_{2',3'}$	$J_{2'',3'}$	$J_{3',4'}$	$J_{4',5'}$	$J_{4',5''}$	$J_{5',5''}$	$J_{2',P2'}$	$J_{3',P3'}$	$J_{4',p5'}$	$J_{5',P5}$	$J_{5'',P5''}$
Ap	30 °C	5 8	-	-	5 4	-	3 2	6 3		a	8 7	-	-	-	-
	60 °C	6 0	-	-	5 2	-	2 9	7 3		a	a	-	-	-	-
pGp	30 °C	5 3	-	-	5 4	-	3 8	2 2	5 2	9 0	8 7	7 1	1 0	5 1	5 1
	60 °C	5 2	-	-	5 8	-	2 8	3 9	4 4	1 1 9	8 4	7 7	a	3 5	5 1
p(dC)2′p	30 °C	6 0	6 0	1 3 5	5 3	6 5	5 0	4 6		a	-	-	-	5 1	
	60 °C	6 2	6 2	1 4 0	4 7	6 7	3 9	6 1		a	-	-	-	7 8	
pC3′p	30 °C	4 2	-	-	5 5	-	a	3 9	2 8	1 1 4	-	-	-	4 5	4 3
	60 °C	4 3	-	-	5 4	-	a	2 3	4 7	1 0 6	-	-	-	5 6	3 1

* resolution 1 Hz/point
a. could not be determined

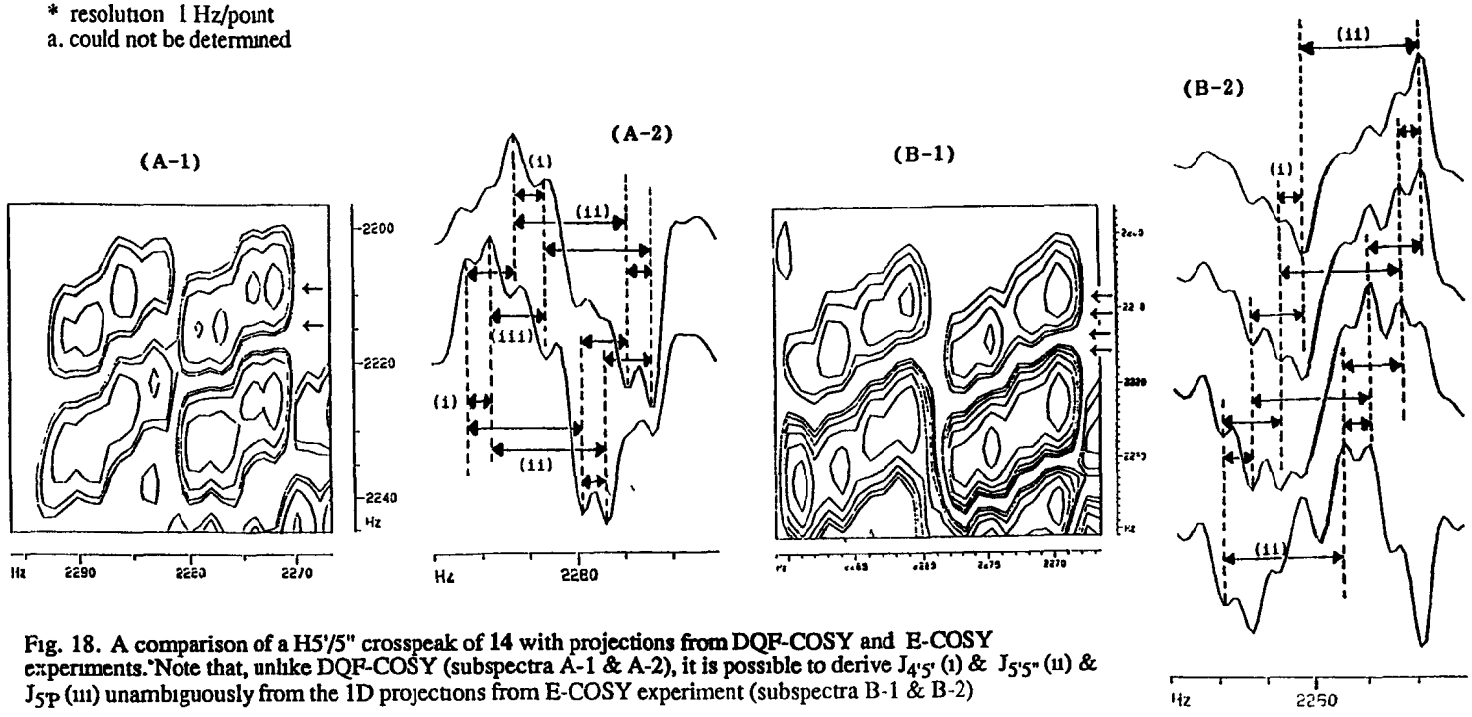

Fig. 18. A comparison of a H5′/5″ crosspeak of 14 with projections from DQF-COSY and E-COSY experiments. Note that, unlike DQF-COSY (subspectra A-1 & A-2), it is possible to derive $J_{4'5'}$ (I) & $J_{5'5''}$ (II) & $J_{5'P}$ (III) unambiguously from the 1D projections from E-COSY experiment (subspectra B-1 & B-2)

(D) Conformation across the glycosidic bond At 500 MHz, 2D NOESY and ROESY experiments were performed on tetramers **13** and **14** at different concentrations (1 8 mM and 6 4 mM for **13**, and 1 8 mM, 6 4 mM and 11 9 mM for **14**) Typical examples of these NOESY and ROESY spectra are shown in Figs 9, 10, 11 and 12 From these experiments, the orientation of the base (*syn* or *anti*) with respect to its own sugar ring was determined A nucleoside is considered to prefer an *anti* conformation when a strong NOE between its H8 (H6) and its H2' together with a weak NOE between its H8 (H6) and its H1' proton is observed In both **13** and **14**, at low concentration (1 8 mM), the H8 of adenosine shows a strong NOE with its H2'/H3' suggesting an *anti* conformation, at higher concentration (6 4 mM for **13**, 6 4 mM and 11 9 mM for **14**) the H8A only showed NOE with its H1' proton implying that it has a *syn* conformation The H8 of guanosine and H6 of the 2'→ 5' linked residue in both tetramers show strong NOE with their respective H2' and H3' at both low and high concentration, which suggests an *anti* conformation For the 3'→ 5' linked cytosine in tetramer **13** we could observe NOE between its H6 and its H1', H2' and H3' protons at 1 8 mM concentration suggesting an *anti* conformation In all other cases for the 3'→ 5' linked cytosine in tetramer **13** and **14** we could only observe NOE between its H6 and its H1' proton or no NOE at all between the base and the sugar

(E) Conformation of C4´-C5´ bond (γ) The conformational behaviour of C4'-C5' bonds is monitored by means of the measurement of the vicinal ^1H-^1H coupling of $J_{4'5'}$ and $J_{4'5''}$ The population of the γ^+ rotamer can be calculated[22] using equation 3

$$\%\gamma^+ = 100(13\ 3 - (J_{4'5'} + J_{4'5''}))/9\ 7 \qquad (3)$$

The data in Tables 10 and 11 show that most residues are highly populated with γ^+ In both tetramers an increase in temperature has a considerable effect on the γ^+ population of the 2'→5' linked residue In tetramer **14** there is only a small change in γ^+ population of the other sugar residues Note that in tetramer **13** there is also a change in γ^+ populations for the 5´-terminal adenosine residue (72% at 30 °C to 62% at 60 °C) and the guanosine residue (61% at 30 °C to 52% at 60 °C) The observed decrease of γ^+ populations when temperature is increased (especially for the 2'→5' linked residues) can be attributed to a destacking of the molecule along the A3'→ 5'G2'→ 5'dC (or C) nucleotides in the tetramers, it is however more preponderant in the case of **13**

Table 10 Calculation of $\%\gamma^+$, $\%\beta^t$ and %N from coupling constants observed at 500 MHz spectra of **13**

	A-residue		G-residue		dC-residue [2´→5´]		C-residue [3´→5´]	
	30 °C	60 °C	30 °C	60 °C	30 °C	60 °C	30 °C	60 °C
$\%\gamma^+$	72	62	61	52	90	74	68	65
$\%\beta^t$	-	-	72	81	99	85	80	80
%N*	30	28	38	39	63	56	54	52
%N#	24	21	34	27	53	48	-	-

* calculated using formula %N = 100((7 9 - $J_{1'2'}$)/6 9) for ribo-sugars and %N = 100(1 - (($J_{1'2'}$+$J_{1'2''}$-9 8)/5 9)) for deoxyribo-sugar; # calculated using PSEUROT program, γ^+ calculated using formula $\%\gamma^+$= 100(13 3-($J_{4'5'}$+$J_{4'5''}$))/9 7, β^t calculated using formula $\%\beta^t$= 100(25 5-($J_{H5'P5'}$+$J_{H5''p5'}$))/20 5

(F) Conformation of C5´-O5´ bond (β) The rotamer population about the C5'-O5' bond can be monitored by the ^1H-^{31}P coupling constants $J_{H5'P5'}$ and $J_{H5''P5'}$ The population of the preferred trans conformer (β^t) can be estimated from the J_{HP} couplings using equation 4[23]

$$\%\beta^t = 100(25\ 5 - (J_{H5'P5'} + J_{H5''P5'}))/20\ 5 \qquad (4)$$

Tables 10 and 11 show the poulation of β^t rotamer for **13** and **14** calculated from the ^1H-^{31}P coupling constants The trans rotamer is highly populated for all residues This preference for the trans conformation is a general feature for stacked oligoribonucleotides In both tetramers the 2'→5' linked residue is more populated than the rest and it is also the one that is most affected by an increase in temperature

Conclusion. Comparison of conformations between **13** and **14** by 500 MHz ^1H- and 202 MHz ^{31}P-NMR spectroscopy clearly showed that they exist as unaggregated monomers with intramolecular stacking along the A3'→ 5'G2'→ 5'dC axis in **13** or A3'→ 5'G2'→ 5'C axis in **14** at concentration below 1 8 mM (Fig 19a)

Table 11 Calculation of $\%\gamma^+$, $\%\beta^t$ and %N from coupling constants observed at 500 MHz spectra of **14**

	A-residue		G-residue		C-residue [2′→5′]		C-residue [3′→5′]	
	30 °C	60 °C	30 °C	60 °C	30 °C	60 °C	30 °C	60 °C
$\%\gamma^+$	77	74	55	52	97	79	78	75
$\%\beta^t$	-	-	78	80	94	73	72	70
%N*	36	33	38	29	84	70	52	52
%N#	28	28	34	29	81	73	-	-

* calculated using formula %N = 100((7 9 - $J_{1'2'}$)/6 9), # calculated using PSEUROT program, γ^+ calculated using formula $\%\gamma^+ = 100(13\ 3\text{-}(J_{4'5''}+J_{4'5''}))/9\ 7$, β^t calculated using formula $\%\beta^t = 100(25\ 5\text{-}(J_{H5'P5''}+J_{H5''p5'}))/20\ 5$

Severe aggregation of these tetramers, leading to vertically stacked structure, however takes place at a higher concentration (Fig 19b) This aggregation at a higher concentration does not however seriously disrupt the geometry of the monomer structures that are found in dilute solution, except for the transition from *anti* to *syn* glycosyl torsion for the 5'-terminal A, as evident by the analysis of J coupling constants, NOESY and ROESY spectra Note that in our earlier studies with naturally-occuring branched tetramer U3 p5′$A^{2'p5'G}_{3'p5'C}$24 involved in the pre-mRNA processing of mRNA (Splicing), such intermolecularly stacked structure was not detectable up

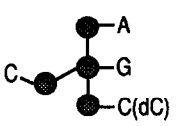

(a) A3'→5'G2'→5'C(dC) stacked model for branched tetramer **13** or **14** at ~1 8 mM solution

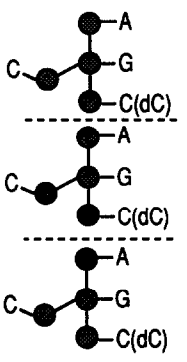

(b) Intermolecular vertically stacked structure for branched tetramer **13** or **14** at ~3 mM solution

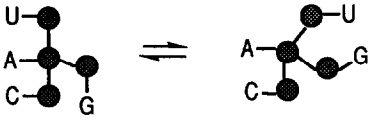

(c) 3'→5' stacked model for U3'p5'$A^{2'p5'G}_{3'p5'C}$ (see ref 24)

Figure 19

to 5 mM concentration[24] The presence of intramolecular stacking along the A3'→ 5'G2'→ 5'dC axis in A3 p5′$G^{2'p5'[dC]}_{3'p5'C}$ (**13**) was also clearly absent in naturally-occurring branched tetramer U3′p5′$A^{2'p5'G}_{3'p5'C}$ in which we

observed a two-state stacked structure in equilibrium along the [U3'→ 5'A2'→ 5'C] ⇄ [U3'→ 5'A2'→ 5'C] axis (Fig 19c)[24] that are reminiscent of A-RNA type structure In both **13** and **14**, G2'→ 5'dC(C) stacking is absolutely preferred unlike the counterpart A2'→ 5'G in U3'p5'$A^{2'p5'G}_{3'p5'C}$ [24] Note that this G2'→ 5'dC(C) stacking and predominant S conformation of the pentose of the branch-point G in **13** and **14** is reminiscent of A2'→5'G stacking which we found in the branched trimer $A^{2'p5'G}_{3'p5'C}$ [19] This unusual 2'→ 5' stacked structure found for **13** may actually be a representative of the structure that actually exists in the branched RNA-msDNA in *Stigmatella aurantiaca* (Myxobacteria), and therefore is not recognized and digested by the endocellular enzymes which may explain its unusual stability that seems to play a quite important role during the life cycle of myxobacteria[1]

Experimental

Chemistry ^{1}H-NMR spectra were recorded in δ scale with a Jeol FX 90 Q and Bruker AMX 500 spectrometer at 90 and 500 MHz, respectively, using TMS (0 0 ppm) or residual HOD peak (set at δ4 7 ppm) as the internal standards ^{31}P-NMR spectra were recorded (in δ scale) at 36 MHz and 202 MHz in the same solvent using 85 % phosphoric acid or cAMP as the external standard TLC was carried out using Merck pre-coated silica gel F_{254} plates in the following solvent systems (A) methanol-dichloromethane (5 95, v/v), (B) methanol-dichloromethane (10 90, v/v), (C) methanol-dichloromethane (20 80, v/v) The short column chromatographic separations were carried out using Merck G60 silica gel DEAE- Sephadex A-25 from Pharmacia was used for the anion excange chromatography After purification on DEAE-Sephadex column, the ammonium counterions in branched tetramers **13** and **14** were replaced with Na^+ by passing the compounds through a Dowex (Na^+ form) column then were repeatedly freezy-dried from ^2H_2O

Synthesis of the dimer 3: Diester block **1** (0 192 g, 0 19 mmol) and dihydroxy block **2** (0 129 g, 0 21 mmol) were repeatedly coevaporated with dry pyridine then dissolved in 3 ml of the same solvent, 1-mesitylenesulfonyl-3-nitro-1,2,4-triazole (MSNT) was added (0 171g, 0 58 mmol) and the mixture stirred for 45 min Usual work-up and column chromatography gave compound **3** (0 211 g, 75 %) R_f 0 49 (System B) ^{31}P-NMR ($CDCl_3$ + DABCO) -7 81, -8 49

Synthesis of the dimer 4: Dimer **3** (0 244 g, 0 16 mmol) was dissolved in chloroform (16 ml) and cooled to 0 °C To this solution 0 1 N trichloroacetic acid (16 ml) in 4% etanol/chloroform was added and stirred at 0 °C for 8 h, then work-up with saturated sodium bicarbonate and chromatography yielded dimer **4** (0 12 g, 58 %) R_f 0 30 (system A) ^{31}P-NMR ($CDCl_3$) -7 15, -7 76

Preparation of the fully protected trimer 6: Compound **3** (0 31 g, 0 21 mmol), compound **5** (0 40 g, 0 63 mmol) and 1,2,3,4-tetrazole were dissolved in dry acetonitrile (10 ml) and stirred for 70 min under dry condition, then 0 1 M iodine solution in THF pyridine water (7 2 1, v/v/v) was added until the iodine colour remained unchanged After 20 min, the reaction mixture was worked up in the usual way, product was purified by short column chromatography with 1% pyridine in the eluant system Yield 0 34 g (79 %) R_f 0 40 (System B) ^{31}P-NMR ($CDCl_3$ + DABCO) -1 93, -2 34, -2 49, -2 88, -8 52, -8 67, -8 79

Removal of the β-cyanoethyl protecting group from compound 6: Compound **6** (0 34 g, 0 17 mmol) was dissolved in dry pyridine (6 8 ml) then dry triethylamine (0 47 ml, 3 4 mmol) was added and the mixture stirred under dry conditions After 6 h, another 10 equiv of triethylamine was added After 11 h of total reaction time, volatile materials were evaporated, the resulting foam was subjected to short column chromatography with triethylamine in the eluant, followed by precipitation from cold hexane to give **7** (0 31 g, 89 %) R_f 0 48 (System C) ^{31}P-NMR ($CDCl_3$ + triethylamine) -0 76, -1 12, -8 28, -8 62

Removal of the pixyl protecting group from compound 7: Deprotection of compound **7** (0 31 g, 0 15 mmol) was performed in the same way as for compound **4** but it took 20 min for completion After short column chromatography, the pure partially protected trimer **8** was washed with 1 0 M TEAB buffer and precipitated from hexane (0 2 g, 74 %) R_f 0 44 (System C) ^{31}P-NMR ($CDCl_3$) 0 59, -0 10, -7 52, -7 64

Preparation of tetramer 11: To a mixture ot compound **8** (0 14 g, 0 078 mmol), compound **9** (0 22 g, 0 42 mmol) and tetrazole (0 148 g, 2 11 mmol) was added dry acetonitrile (5 ml) in an argon atmosphere and the turbid mixture was stirred for 50 min Oxidation was performed as for compound **6**, but iodine was dissolved in THF pyridine water (8 1 1 v/v/v) After usual work-up, the product was purified by short column chromatography followed by washing with 1 0 M TEAB buffer Yield 0 15 g (86 %) R_f 0 60 (System C) ^{31}P-NMR ($CDCl_3$) -0 37, -0 59, -0 98, -1 03, -1 17, -1 25, -1 34, -1 46, -1 68, -7 49, -7 64, -7 76, - 7 86

Deprotection of tetramer 11 Compound **11** (121 mg, 0 054 mmol) and *syn*-4-nitrobenzaldoxime (90 mg, 0 54 mmol) were dissolved in dioxane-water mixture (10 ml, 1 1 v/v) and 1,1,3,3-tetramethylguanidine (0 068 ml, 0 54 mmol) was added After 20 h, 32% ammonia solution (18 ml) was added and stirred at 52 °C for 38 h, then volatile matters were removed *in vacuo*, the residue was treated with 80% acetic acid (50 ml) for 5 h Volatile materials were removed, followed by coevaporations with water to remove traces of acid, residue was dissolved in water and washed with dichloromethane The aqueous phase was evaporated then dissolved in a few ml of water and applied to a DEAE-Sephadex A-25 column, eluted with linear gradient of ammoniumbicarbonate buffer (0 0M - 0 25M, 0 25M - 0.5M, 500 ml each) Appropriate fractions were pooled, evaporated and coevaporated with distilled water until complete removal of the buffer salt to give **13** Yield 709 A_{260} units (33 %)

Synthesis of tetramer 12 Dimer **4** (0 115 g, 0 09 mmol), phosporoamidite **10** (0 39 g, 0 63 mmol) and tetrazole (0 46 g, 6 3 mmol) were dissolved in dry acetonitrile (5 ml) for 50 min Oxidation as for compound **9** and usual work-up followed by short column chromatography afforded compound **12** Yield 0 168 g (84 %) R_f 0 45 (System B) ^{31}P-NMR ($CDCl_3$) 0 24, 0 15, -0 59, -0 63, -0 68, -0 78, -0 90, -1 03, -1 17, -1 22, -1 34, -1 66, -1 88, -7 59,-7 64, -7 69, -7 76, -7 98, -8 11

Deprotection of tetramer 12 0 14 g (0 063 mmol) of the tetramer was treated in the similar way as described for the deprotection of compound **11** Purification on a DEAE-Sephadex A-25 colum with the same eluant system gave 924 A_{260} units of **14** (38 %) *NMR sample preparations for 500 MHz NMR spectroscopy* The NMR samples were lyophilized twice from 99 8% D_2O. The samples were then dissolved in 0 5 ml of 99 96% D_2O and transferred into 5 mm tubes The sample concentration was 1 8 mM for all experiments The 2D NOESY which was run at 1.8 and 6 4 mM for **13** and at 1 8, 6 4 and 11 9 mM for **14** *NMR aquisitions* All NMR spectra were recorded on a Bruker AMX-500 spectrometer ^{1}H-NMR spectra were collected with 32K data points and zero filled to 64K data points A trace of dry acetonitrile was added as an internal reference for chemical shift measurements (δ 2 00 ppm) The ^{31}P-NMR spectra were acquired with 8K data points and zero filled to 16K The ^{31}P chemical shifts are relative to 3'5'-cyclic AMP as an external reference (δ -2 1 ppm) The following 2D NMR techniques were employed (i) HOHAHA[15] These spectra were recorded in the phase-sensitive mode at 35°C according to the method of Bax et al The MLEV-17 sequence is applied for mixing, and two different power levels were used for exchange and spin-lock A mixing time of 350 ms was used in all our HOHAHA spectra For each experiment we recorded 512 spectra of 2K real points (72 scans for both **13** and **14**), using a sweep width of 4000 Hz Quadrature detection in t_1 was achieved with TPPI The t_1 domain was zero-filled to 1K, and a sinesquare (π/4) window was applied in both dimensions before Fourier transformation (ii) DQF-COSY[16] These experiments were performed in the phase-sensitive mode at 30 °C and 60 °C with and without ^{31}P decoupling In each case, we collected 512 spectra of 4K real data points (72 scans for both **13** and **14**), using a sweep width of 4000 Hz Quadrature detection in t_1 was achieved with TPPI. The t_1 domain was zero-filled to 2K, and a sinesquare (π/4) window was applied in both dimensions before Fourier transformation (iii) ^{1}H-^{31}P correlation spectroscopy[26] These experiments were run in absolute value mode J(XH) = 6 Hz was used to calculate the delays 256 experiments were recorded, for each experiment we recorded 96 scans of 1K real data points The spectral range used was 1000 Hz in the t_2 direction and 4000 Hz in the t_1 The spectra was zero-filled to 512 data points in t_1 and a sinesquare (π/4) window was applied in both dimensions before Fourier transformation (iv) E-COSY[17] We recorded E-COSY experiments in the phase-sensitive mode at 60°C with and without ^{31}P decoupling The experiments were run to help to extract the coupling constants that were impossible to get from DQF-COSY due to overlap of resonances at 60°C In each case, we collected 512 spectra of 4K data points (96 scans for both **13** and **14**), using a sweep width of 4000 Hz Quadrature detection in t_1 was achieved with TPPI The t_1 domain was zero-filled to 2K, and a sinesquare (π/4) window was applied in both dimensions before Fourier transformation (v) NOESY We recorded NOESY spectra on both tetramers at different concentrations (1 8 mM and 6 4 mM for **13**, 1 8 mM, 6 4 mM and 11 9 mM for **14**) at 30 °C with mixing time of 900 ms, 512 t_1 increments with 2K data points (72 scans for all experiments except those run at 1 8 mM were we used 96 scans) and a sweep width of 4000 Hz Quadrature detection in t_1 was achieved with TPPI The t_1 domain was zero-filled to 1K, and a sinesquare (π/3) window was applied in both dimensions before Fourier transformation (vi) ROESY[25] The experiments were recorded in the phase-sensitive mode at 30°C A CW spinlock was used for mixing The mixing time was 900 ms. For each experiment we recorded 512 spectra of 2K real points (72 scans for both **13** and **14**), using a sweep width of 4000 Hz Quadrature detection in t_1 was achieved with TPPI The t_1 domain was zero-filled to 1K, and a sinesquare (π/4) window was applied in both dimensions before Fourier transformation

Acknowledgements: Authors thank Swedish Board for Technical Development and Swedish Natural Science Research Council for generous financial support Authors also thank Wallenbergs Stiftelsen, University of Uppsala and Swedish Research Council (FRN) for grants for the purchase of the 500 MHz NMR spectrometer

References

+ On leave from Central Research Laboratory, University Medical School of Pécs, Hungary

1 (a) T Furuichi, A Dhundale, M Inouye and S Inouye, *Cell*, **48**, 47 (1987); (b) T Furuichi, S Inouye and M Inouye, *Cell*, **48**, 55 (1987)
2 (a) M. Sekine and T Hata, *J Am Chem Soc* , **107**, 5813 (1985), (b) M Sekine, J Heikkilà and T Hata, *Tetrahedron Lett* , **28**, 5691 (1987)
3 (a) R Kierzek, D. Kopp, M Edmonds and M Caruthers, *Nucleic Acids Res* , **14**, 4751 (1986), (b) J-M Vial, N Balgobin, G Remaud, Á Nyilas and J Chattopdhyaya, *Nucleosides & Nucleotides*, **6**, 209 (1987), (c) S Huss, G Gosselin and J-L. Imbach, *Tetrahedron Lett* , **28**, 415 (1987), (d) J-M Vial, G Remaud, N Balgobin and J Chattopadhyaya, *Tetrahedron*, **43**, 3997 (1987), (e) X-X. Zhou, Á Nyilas, G Remaud and J Chattopadhyaya, *Tetrahedron*, **43**, 4687 (1987); (f) S Huss, G Gosselin and J-L Imbach, *J Org Chem* , **53**, 499 (1988), (g) X-X Zhou, G Remaud and J Chattopadhyaya, *Tetrahedron*, **44**, 6471 (1988) (h) N Balgobin, A Földesi, G Remaud and J Chattopadhyaya, *Tetrahedron*, **44**, 6929 (1988), (i) G. Remaud, N Balgobin, A Sandström, J-M Vial, L H Koole, H M Buck, A F Drake, X-X Zhou and J Chattopadhyaya, *J Biochem & Biophys Methods*, **18**, 1 (1989)
4 A Földesi, N Balgobin and J Chattopadhyaya, *Tetrahedron Lett* **30**, 881 (1989)
5 A Sandström, M. Kwiatkowski and J. Chattopadhyaya, *Acta Chem Scand* , **B39**, 273 (1985)
6 J Chattopadhyaya and C B Reese, *Tetrahedron Lett.*, 5059, **1979**
7 S S Jones, B. Rayner, C B Reese, A Ubasawa and M Ubasava, *Tetrahedron*, **36**, 3075 (1980)
8 C B Reese, *Tetrahedron*, **34**, 3143 (1978)
9 N D Sinha, J Biernat and H Köster, *Tetrahedron Lett* , **24**, 5843 (1983)
10 L McBride and M Caruthers, *Tetrahedron Lett* , **24**, 245 (1983)
11 R. W Adamiak, M Z Barciszewska, E Biala, K. Grzéskowiak, R Kierzek, A Kraszewski, W T Markiewicz and M. Wiewiórowski, *Nucleic Acids Res.*, **3**, 3397 (1976)
12 (a) J Chattopadhyaya and C B Reese, *J Chem Soc Chem Commun* , 639, **1987**, (b) M Kwiatkowski and J Chattopadhyaya, *Chemica Scripta*, **20**, 139 (1982)
13 M Kwiatkowski, J Heikkilà, S Bjorkman, H Seliger and J. Chattopadhyaya, *Chemica Scripta*, **22**, 30 (1983)
14 B.E. Griffin, M Jarman and C B Reese, *Tetrahedron*, **24**, 639 (1968)
15 (a) D G Davies, A Bax, *J Am Chem Soc* , **107**, 2802 (1985), (b) D G Davies, A Bax *J Am Chem Soc* , **107**, 7197 (1985)
16 (a) D Neuhaus, G Wagner, M Vasak, J H R. Kagi, K Wuthrich, *Eur J Biochem* , **151**, 257 (1985), (b) K Wuthrich in "NMR of Proteins and Nucleic Acids", Wiley, New York (1986)
17 (a) C Griesinger, O W. Sorensen, R R Ernst, *J Am Chem Soc* , **107**, 6394 (1985), (b) C Griesinger, O W Sorensen, R R Ernst, *J Chem Phys* , **64**, 6837 (1986), (c) C Griesinger, O W Sorensen, R R Ernst, *J Magn Reson* , **75**, 474 (1987)
18 D B Davies in "Progress in NMR Spectroscopy", J W Emsley, J Feeney, L H Sutcliffe, Eds Vol 12, p 135 (1978)
19 (a) G Remaud, J-M Vial, A Nyilas, N Balgobin, J Chattopadhyahya, *Tetrahedron*, **43**, 947 (1987), (b) J-M Vial, G. Reamaud, N Balgobin and J Chattopadhyaya, *Tetrahedron*, **43**, 3997 (1987), (c) L H Koole, N. Balgobin, H M Buck, W H A Kuijpers, A Nyilas, G Remaud, J-M Vial and J Chattopadhyaya, *Recl Trav Chim Pays-Bas*, **107**, 663 (1988)
20 (a) F A A M de Leeuw, C Altona, *J Comp Chem* , **4**, 428 (1983), (b) F A A M de Leeuw, C Altona, *Quant Chem Progr Exch* 463, University of Indiana at Bloomington (1983)
21 (a) J Doornbos, C T J Wreesmann, J H van Boom, C Altona, *Eur J Biochem* , **131**, 571 (1983), (b) F A.A M de Leeuw, C Altona, *J Chem Soc Perkin Trans 2*, 375, **1982**, (c) L J Rinkel, C Altona, *J Biomol Struct Dyns* , **4**, 621 (1987)
22 C Altona, *Recl Trav Chim Pays-Bas*, **101**, 413 (1982)
23 P P Lankhorst, C A G Haasnoot, C. Erkelens, C Altona, *J Biomol Struct Dyn* , **1**, 1387 (1984)
24 (a) C Glemarec, M Jaseja, A Sandström, L Koole, P Agback and J Chattopadhyaya, *Tetrahedron*, **47**, 3417 (1991), (b) X-X Zhou, A Nyilas, G Remaud and J. Chattopadhyahya, *Tetrahedron*, **44**, 571 (1988), (c) G Remaud, N Balgobin, C Glemarec, and J Chattopadhyahya, *Tetrahedron*, **45**, 1537 (1989), (d) A Sandström, G Remaud, J-M Vial, X-X Zhou, A Nyilas, N Balgobin and J Chattopadhyaya, *J Chem Soc Chem Commun* , 542, **1988**
25 A Bax, D G Davies, *J Magn Reson* , **63**, 207 (1985)
26 A Bax, G A Morris, *J Magn Reson* , **42**, 501 (1981)
27 (a) C Altona, M Sundaralingam, *J Am Chem Soc* , **94**, 8205 (1972) (b) C Altona, M Sundaralingam, *J Am Chem Soc* , **95**, 2333 (1973)